

# Supplementary Information for “Mechanical forcing of the North American monsoon by orography”

William R. Boos<sup>1,2,\*</sup> and Salvatore Pascale<sup>3</sup>

<sup>1</sup>Department of Earth and Planetary Science, University of California, Berkeley, USA

<sup>2</sup>Climate and Ecosystem Sciences Division, Lawrence Berkeley National Laboratory, USA

<sup>3</sup>Department of Physics and Astronomy, University of Bologna, Italy

\*billboos@alum.mit.edu

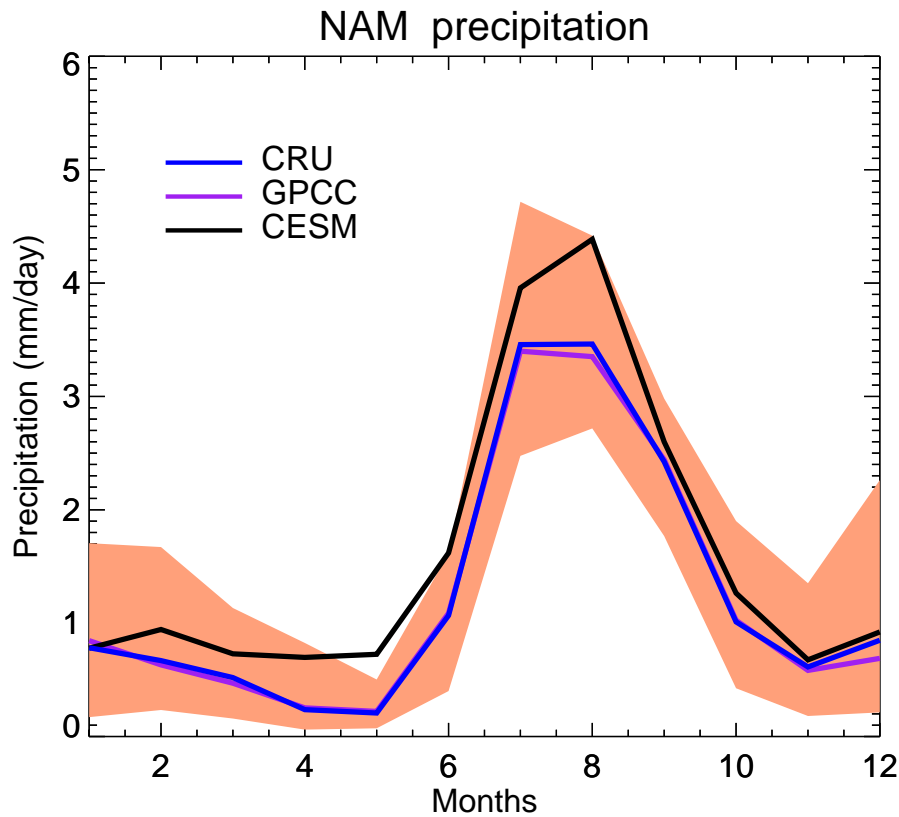


**Figure 1.** The seasonal cycle of NAM precipitation simulated by the high-resolution GCM falls within the range of observed interannual variability, lacking the wet autumn bias commonly seen in lower-resolution ocean-atmosphere coupled GCMs. Lines show the seasonal cycle of monthly precipitation averaged over the North American monsoon land domain and over the period 1980-2009 in two observational datasets (the Climatic Research Unit gridded Time Series in blue [CRU]<sup>1,2</sup>, the Global Precipitation Climatology Centre [GPCC]<sup>3</sup> dataset version 7, in purple), and in the Control GCM simulation (CESM; black). Shading bounds the 5<sup>th</sup> and 95<sup>th</sup> percentiles of GPCC interannual variability. The domain used for averaging is the same as in Pascale et al. (2017)<sup>4</sup>.

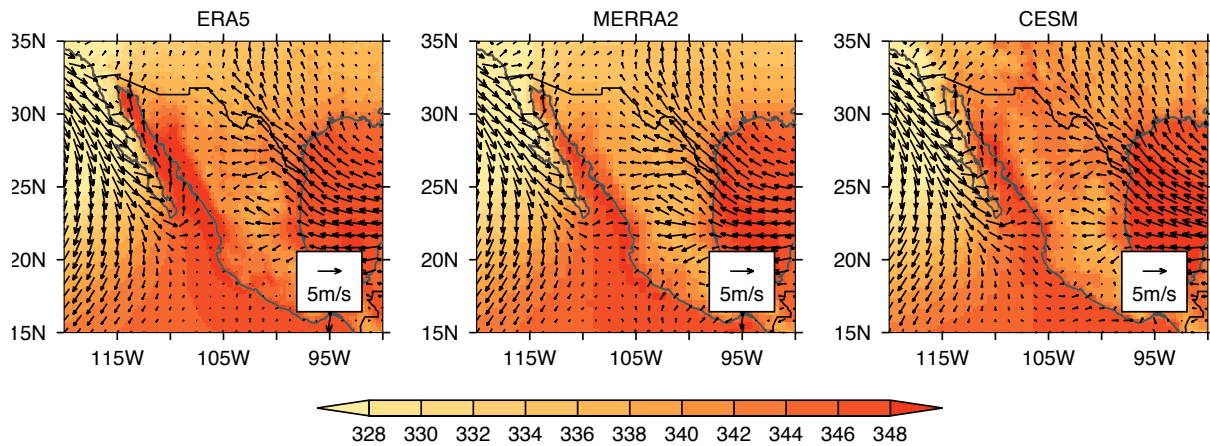


**Figure 2. The high-resolution GCM captures the northward low-level wind and the tongue of high moist static energy (MSE) air along the Gulf of California.** Vectors show the near-surface horizontal wind, specifically the 10-m wind from both ERA5 (1980-2019 mean) and MERRA2 (1980-2019 mean) and the lowest model level wind from the Control GCM (CESM; roughly 7 hPa above the surface). Shading shows the 2-m MSE, normalized by the specific heat of dry air to cast this variable in units of K.

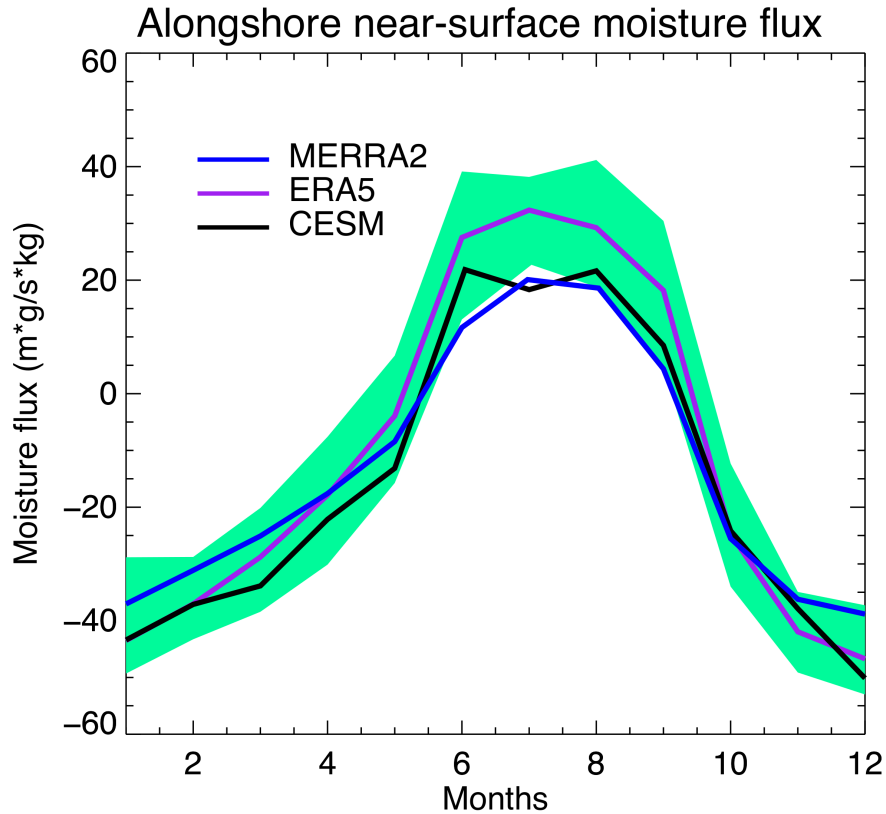


**Figure 3. The high-resolution GCM realistically represents the seasonal cycle of the along-shore moisture flux in the Gulf of California (GoC).** Lines show the coast-parallel component of the 10-m moisture flux in the GoC for 1980-2009 in two reanalyses (MERRA2 in blue and ERA5 in purple) and the lowest model-level moisture flux in the Control GCM (CESM; black, about 7 hPa above the surface). Shading bounds the 5<sup>th</sup> and 95<sup>th</sup> percentiles of ERA5 interannual variability. The coast-parallel direction is 34° counterclockwise from north, and calculations follow the same procedure as in the Supplementary Information of Pascale et al. (2017)<sup>4</sup>.

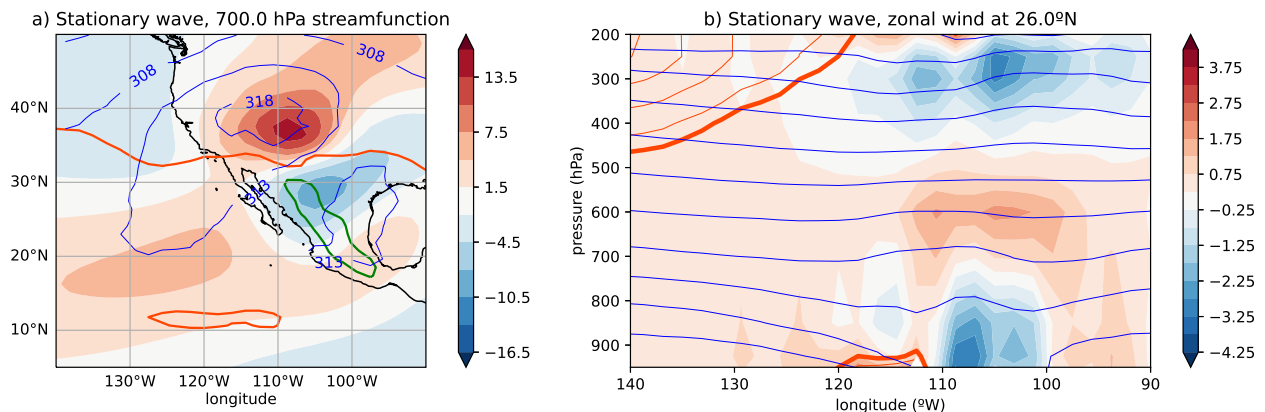


**Figure 4. Linear stationary wave solution.** Same as Fig. 2c, d of the main text, but obtained by scaling the orographic forcing by 0.01 then multiplying the response by 100. The green contour in (a) outlines the forcing, but no orography is masked in (b) because of the rescaling. Isentropes in the forcing region (roughly 100-110°W) do not intersect orography because the orography has been rescaled to be small.

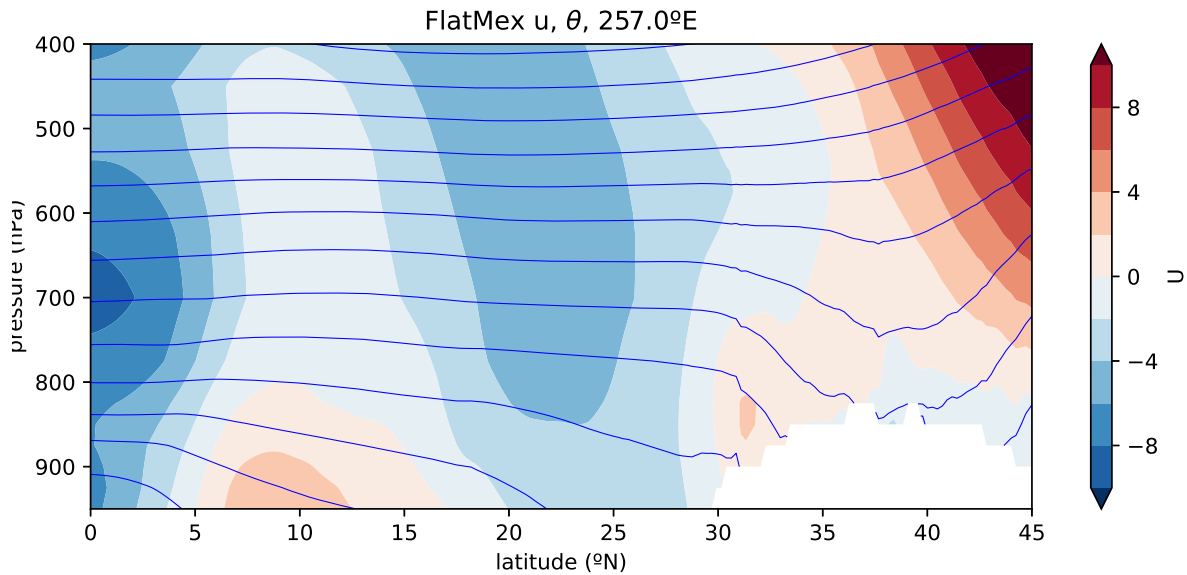


**Figure 5.** Basic state isentropes and zonal wind, illustrating how steady, lower-tropospheric adiabatic flow must be deflected southward to avoid being blocked by the ground. Summer-mean zonal wind (shading,  $\text{m s}^{-1}$ ) and potential temperature (blue contours, interval 5 K) at  $103^\circ\text{W}$  in the FlatMex integration. Orography is masked in white.

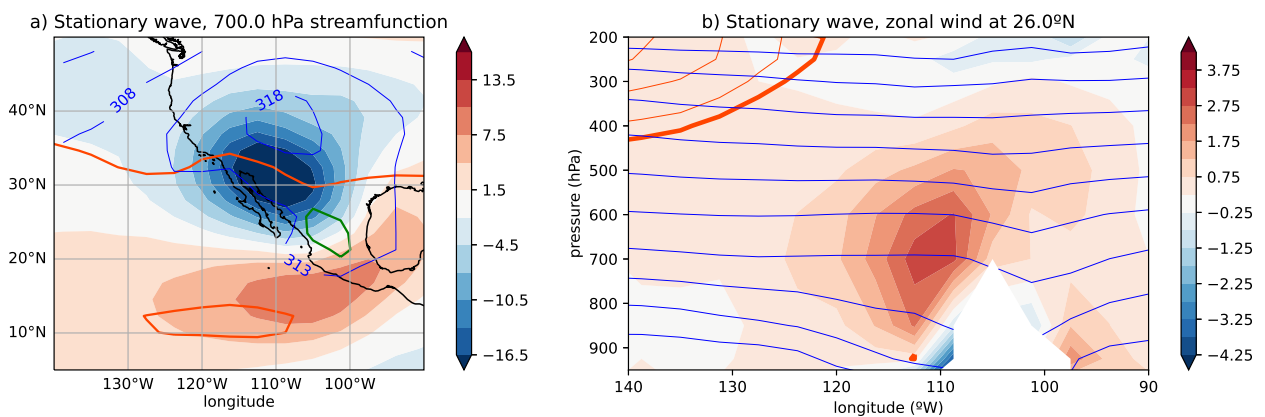


**Figure 6.** Low-resolution stationary wave solution. Same as Fig. 2c, d of the main text, but obtained with the stationary wave model integrated at R30 horizontal resolution (the main text showed solutions at R63 resolution). Note that the total near-surface flow just west of the SMO is westward, unlike in the high-resolution solutions shown in Fig. 2d.

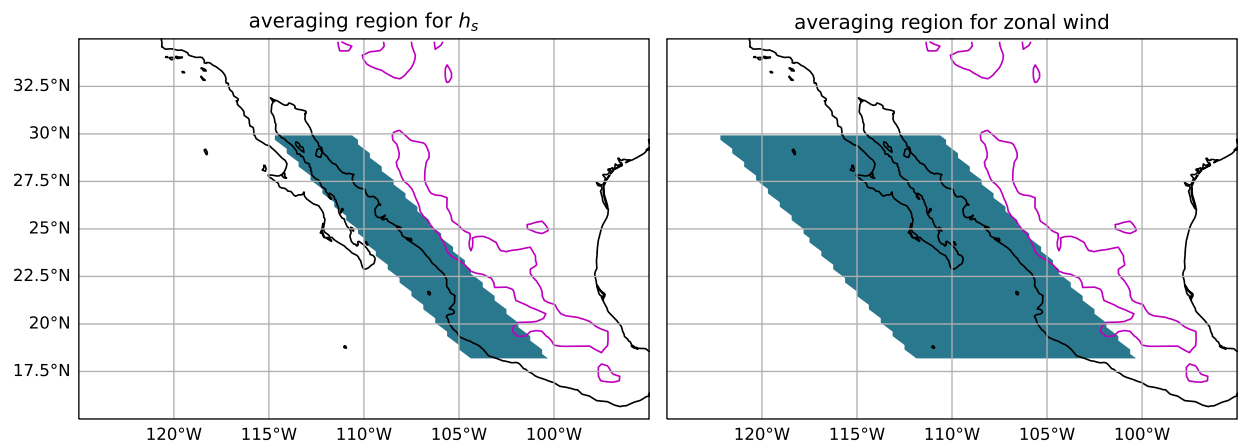


**Figure 7.** Averaging regions for Fig. 3. Regions over which surface air MSE (left panel) and low-level zonal wind (right panel) were averaged in our seasonal cycle diagnostics.

## References

1. Harris, I., Jones, P., Osborn, T. J. & Lister, D. H. Updated high-resolution grids of monthly climatic observations – the CRU TS3.10 Dataset. *Int. J. Clim.* **34**, 623–642 (2013).
2. Harris, I., Osborn, T. J., Jones, P. & Lister, D. Version 4 of the CRU TS monthly high-resolution gridded multivariate climate dataset. *Sci. Data* **7**, 109 (2020).
3. Schneider, U. *et al.* GPCP’s new land surface precipitation climatology based on quality-controlled in situ data and its role in quantifying the global water cycle. *Theor. Appl. Climatol.* **115**, 15–40 (2013).
4. Pascale, S. *et al.* Weakening of the North American monsoon with global warming. *Nat. Clim. Chang.* **7**, DOI: [10.1038/nclimate3412](https://doi.org/10.1038/nclimate3412) (2017).